Biochemical and Biophysical Research Communications 440 (2013) 671–676

Contents lists available at ScienceDirect

Biochemical and Biophysical Research Communications

journal homepage: www.elsevier.com/locate/ybbrc

Identification of the proteins required for fatty acid desaturation in zebrafish (*Danio rerio*)

Yao-Sheng Chen [a,b,c], Wen-I Luo [c], Tsu-Lin Lee [c,d], Steve S.-F. Yu [c,*], Chi-Yao Chang [a,b,*]

[a] Institute of Fisheries Science, National Taiwan University, Taipei 10617, Taiwan
[b] Institute of Cellular and Organismic Biology, Academia Sinica, Taipei 11529, Taiwan
[c] Institute of Chemistry, Academia Sinica, Taipei 11529, Taiwan
[d] Applied and Theoretical Chemistry, Graduate Institute of Applied Science and Technology, National Taiwan University of Science and Technology, Taipei 10607, Taiwan

ARTICLE INFO

Article history:
Received 18 September 2013
Available online 5 October 2013

Keywords:
Cytochrome b5 reductase
Elongase
Fatty acid desaturase
Fluorescence resonance energy transfer
Zebrafish

ABSTRACT

Zebrafish Δ-5/Δ-6 fatty acid desaturase (Z-FADS) catalyzes the cascade synthesis of long-chain polyunsaturated fatty acids (PUFAs), thereby playing a pivotal role in several biological processes. In the current study, we report that the Z-FADS protein exists in close proximity to certain cytochrome b5 reductases (CYB5R2 and 3) and elongases (ELOVL2, 4, 5 and 7) on the endoplasmic reticulum, as determined using fluorescence microscopy and fluorescence resonance energy transfer. HeLa cells co-transfected with zebrafish *fads* and *elovl2*, *4*, and *5* produced docosahexaenoic acid (DHA), as detected by gas chromatography. In addition, immunofluorescence cytochemistry and Western blot data revealed that Z-FADS is present in the mitochondria of HeLa cells. Collectively, our results implicate that Z-FADS, the sole fatty acid desaturase ever been identified in zebrafish, can serve as a universal fatty acid desaturase during lipogenesis.

1. Introduction

Vertebrates are unable to synthesize most polyunsaturated fatty acids (PUFAs) *de novo*, and thus precursor compounds must be obtained from the diet [1,2]. In general, ingestion of plants or algae provides essential fatty acid precursors, such as linoleic acid (LA, 18:2n-6) and α-linolenic acid (ALA, 18:3n-3), and these are used to synthesize long-chain polyunsaturated fatty acids (LC-PUFAs), including arachidonic acid (AA, 20:4n-6), eicosapentaenoic acid (EPA, 20:5n-3), and docosahexaenoic acid (DHA, 22:6n-3). Fatty acids are subjected to multiple desaturation reactions; these reactions are catalyzed by a series of proteins, which include cytochrome b5 reductase (CYB5R) [3], elongase (elongation of very long chain fatty acids, ELOVL), and fatty acid desaturase (FADS). Initially, LA and ALA are converted into acyl-CoAs by CoA ligase; the LA and ALA acyl-CoAs are then desaturated by Δ-6 desaturase, generating γ-linolenic acid (GLA, 18:3n-6) and octadecatetraenoic acid (OTA, 18:4n-3), respectively. These compounds are subsequently extended by two carbons by an elongase to form C_{20} LC-PUFAs; finally, the carboxylate end of each C_{20} LC-PUFA is desaturated by a Δ-5 desaturase to produce AA and EPA, respectively [4] (Fig. S1).

A regio-selective desaturation process is conducted for the formation of a C=C bond. This desaturation process requires CYB5R to provide the electrons necessary for the turnover of FADS, whereas ELOVL performs a two carbon elongation at the carboxylate end of a fatty acid [5]. CYB5R is an NADH-dependent flavin reductase [6] involved in the microsomal electron transport system; this protein exists in both a membrane-bound and a soluble form [7,8]. ELOVL elongase catalyzes condensation, which is believed to be the first step of the elongation cycle. To date, seven homologs of ELOVL (1–7) have been identified, all of which contain multiple transmembrane helices, and reside in the endoplasmic reticulum (ER) [9,5]. ELOVL1, 3, and 6 are responsible for the elongation of long-chain fatty acids (LCFAs), as well as saturated and mono-unsaturated fatty acids. On the other hand, ELOVL5 extends GLA and OTA (Fig. S1). ELOVL2, 4, and/or 5 may be involved in the elongation of LC-PUFAs (including AA and EPA), while ELOVL7 is believed to be involved in the elongation of GLA [10].

FADS is a non-heme diiron enzyme whose desaturation involves the reaction with molecular oxygen at the active site, thereby generating diiron intermediate(s) for the desaturation of LCFA [11,12]. FADS contains an N-terminal cytochrome b5 domain with a heme-binding motif, HPGG, which is essential for desaturation [13,14]. Genes encoding FADS are often clustered together; most vertebrate *fads* clusters contain three genes: *fads1*, *fads2*, and *fads3*. However, only a single *fads* gene has been identified in zebrafish (encoding zebrafish FADS (Z-FADS)), which has been demonstrated to exhibit activity similar to that of both mammalian Δ-5 desaturase and Δ-6

* Corresponding authors. Fax: +886 2 2783 1237 (S.S.-F. Yu). Address: Institute of Cellular and Organismic Biology, Academia Sinica, Taipei 11529, Taiwan. Fax: +886 2 2653 8842 (C.-Y. Chang).
E-mail addresses: sfyu@gate.sinica.edu.tw (S.S.-F. Yu), cychang@gate.sinica.edu.tw (C.-Y. Chang).

0006-291X/$ - see front matter © 2013 Elsevier Inc. All rights reserved.
http://dx.doi.org/10.1016/j.bbrc.2013.09.127

desaturase [15,16]; the zebrafish genome does not contain a gene homologous to *fads3* [4].

In mammals, DHA biosynthesis involves two elongation steps. First, EPA is converted into a 24:5n-3 precursor, which is then converted into tetracosahexaenoic acid (THA, 24:6n-3) by a Δ-6 desaturase. After peroxisomal beta-oxidation, THA is converted into DHA [17] (Fig. S1). In certain marine fish (e.g. *Siganus canaliculatus*) and algae, DHA is synthesized from EPA *via* sequential elongation and desaturation by a Δ-4 desaturase [18] (Fig. S1). In zebrafish, it is suggested that ELOVL4 is involved DHA biosynthesis [19]; however, the identity of the desaturase in this process remains unknown. To identity the relevant desaturase in zebrafish, we used fluorescence resonance energy transfer (FRET) to examine interactions between Z-FADS and ELOVLs or CYB5Rs [20]. We demonstrate here that Z-FADS interacts with CYB5R2, CYB5R3, and ELOVL2, 4, 5 and 7. Furthermore, we reveal that co-transfection with zebrafish *fads* and *elovl2*, *4*, and *5* is sufficient for the formation of DHA in HeLa cells. Our results contribute to the understanding of DHA biosynthesis and the role of Z-FADS in lipogenesis in zebrafish.

2. Materials and methods

2.1. Zebrafish husbandry and cDNA preparation

The wild type zebrafish AB strain was maintained at the Taiwan Zebrafish Core Facility, Academia Sinica, Taiwan. Total RNA was extracted from zebrafish using TRIzol (Invitrogen), and reverse transcribed using SMART™ MMLV Reverse Transcriptase (Clontech).

2.2. Construction of expression vectors

PCR with specific primers (Table S1) was used to amplify the zebrafish *fads*, *elovl*, and *cyb5r* genes. PCR was performed using zebrafish cDNA and *amfiFusion* High Fidelity PCR Master Mix (GenDEPOT). The PCR amplicons were digested with restriction enzymes (Table S1), and then ligated into the corresponding vectors. The eukaryotic expression vectors listed in Table S1 were prepared. The vectors contained the following constructs: (i) pDsRed-monomer-C1-CYB5R: *Discosoma* sp. red fluorescent protein (DsRed) fused to the N-terminus of an CYB5R (1,2 or 3); (ii) pDsRed-monomer-C1-ELOVL: DsRed fused to the N-terminus of an ELOVL (2, 4, 5, or 7); (iii) pcDNA3CF-ELOVL: FLAG tag fused to the C-terminus of an ELOVL; (iv) pHis-ELOVL-FLAG: a poly-histidine tag fused to the N-terminus, and a FLAG tag fused to the C-terminus of an ELOVL; (v) pEGFP-N1-FADS; enhanced green fluorescent protein (EGFP) fused to the C-terminus of Z-FADS; (vi) pEGFP-C1-FADS: EGFP fused to the N-terminus of Z-FADS; and (vii) pcDNA3CF-FADS: FLAG tag fused to the C-terminus of Z-FADS. The identities of all constructs were confirmed by DNA sequencing (MB biotech, Taiwan).

2.3. Fluorescence resonance energy transfer (FRET)

Lipofectamine2000™ (Invitrogen) was used to transfect HeLa cells with vectors encoding Z-FADS, CYB5R, or ELOVL proteins. FRET experiments were designed as the following pairs: (i) HeLa cells co-expressed with EGFP-Z-FADS/Z-FADS-EGFP and DsRed-CYB5R/DsRed-ELOVL; (ii) HeLa cells co-transfected with pcDNA3CF-ELOVLs and pEGFP-N1-FADS/pEGFP-C1-FADS were hybridized with monoclonal anti-FLAG M2 primary antibodies, and then with Rhodamine-conjugated goat anti-mouse IgG secondary antibodies (Millipore); (iii) HeLa cells transfected with pHis-ELOVL-FLAGs were hybridized with rabbit anti-6xHis Tag primary antibodies (LTK BioLaboratories), and then with mouse anti-FLAG M2. The same cells were subsequently hybridized with goat $F(ab')_2$ anti-rabbit IgG tetramethyl rhodamine isothiocyanate (Rhodamine TRITC) (Leinco technologies Inc.) and FITC AffiniPure goat anti-mouse IgG (Jackson ImmunoResearch). All the transfected cells were subjected to a confocal microscopy (Leica, TCS-SP5-AOBS).

The acceptor photobleaching method was used to determine the efficiency of FRET. Green donor fluorescence from EGFP (507 nm) or FITC (519 nm) and red acceptor fluorescence from DsRed (592 nm) or Rhodamine (572 nm) were detected using a confocal microscope (Leica, TCS-SP5-AOBS) and two individual detectors (HyD3, Leica) to prevent the interference from light leakage. The donors were excited at 488 nm; donor fluorescence was de-quenched by bleaching the acceptor with 100% laser power at the appropriate wavelength (i.e., 547 or 557 nm) 25 times, and the resulting increase in donor fluorescence was measured. The distance between the two fluorophores was determined using the following equations:

$$E = \left(\mathrm{Donor}_{\mathrm{post}} - \mathrm{Donor}_{\mathrm{pre}}\right)/\mathrm{Donor}_{\mathrm{post}}$$

$$E = R_0^6/\left(R_0^6 + r^6\right)$$

where E is the energy transfer efficiency, $\mathrm{Donor}_{\mathrm{post}}$ is the fluorescence intensity of the donor after photobleaching, $\mathrm{Donor}_{\mathrm{pre}}$ is the fluorescence intensity of the donor before photobleaching, and R_0 is the 50% FRET distance between two fluorophores.

2.4. Immunofluorescence cytochemistry (IFC)

HeLa cells were transfected with either pEGFP-N1-FADS or pEGFP-C1-FADS. At 18 h after transfection, the cells were fixed and incubated with either rabbit anti-COX IV (GeneTex) (which specifically recognizes mitochondrial cytochrome c oxidase (COX)) or rabbit anti-ERp57 (GeneTex) (which specifically recognizes ERp57, a protein disulfide isomerase in the endoplasmic reticulum (ER)). Cells were subsequently incubated with the goat $F(ab')_2$ anti-rabbit IgG Rhodamine TRITC secondary antibody (Leinco Technologies). Fluorescence was monitored using an Inverted Fluorescent Microscope (Zeiss, Axiovert 200M). Cell nuclei were stained with 4′,6-diamidino-2-phenylindole (DAPI) (Invitrogen).

2.5. Isolation of mitochondria and Western blotting

The mitochondrial membrane fraction of cells expressing FLAG-tagged Z-FADS was isolated as described previously, with some modifications [21]. Briefly, at 18 h after transfection with pcDNA3CF-FADS, HeLa cells were washed, collected, and resuspended in NKM buffer. Cells were subsequently pelleted and resuspended in homogenization buffer. The cells were then homogenized on ice by passing them through a 1 mL syringe with a 261/2 G needle 20 times. After centrifugation, pellets containing the mitochondria were collected and resuspended in a mitochondrial suspension buffer.

For Western blot analysis, the mitochondrial membrane fraction was separated by SDS–PAGE and then transferred to a membrane. Rabbit anti-COX IV and mouse anti-FLAG M2 were used as primary antibodies. Rabbit anti-Lamin A/C (GeneTex), which recognizes Lamin A/C on the nuclear lamina, was used as a negative control. Secondary antibodies (goat anti-rabbit IgG (Sigma) or goat anti-mouse IgG (Dako)) conjugated to alkaline phosphatase were used, and proteins were visualized by NBT/BCIP staining (ThermoScientific).

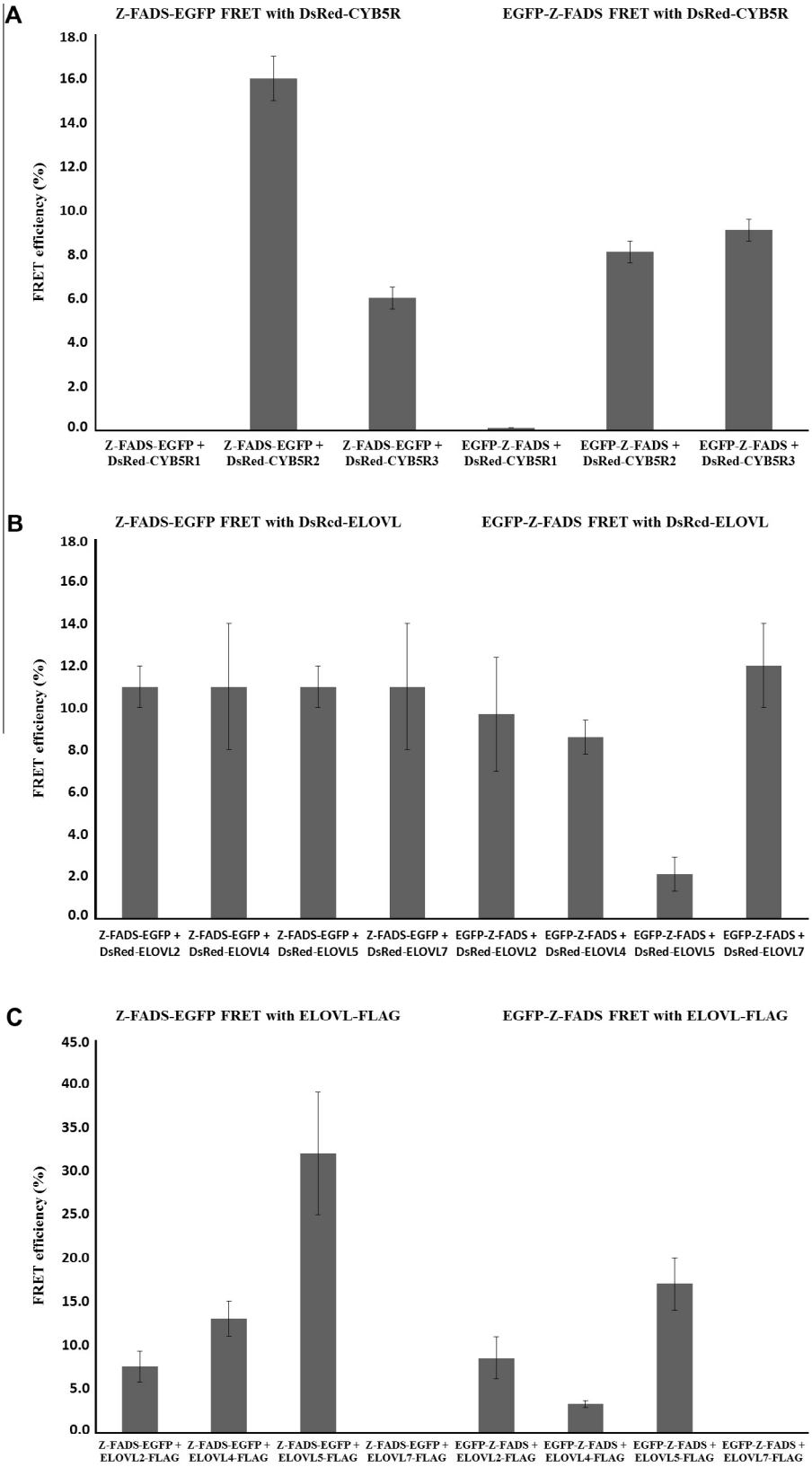

Fig. 1. Fluorescence resonance energy transfer (FRET) between Z-FADS and CYB5R or ELOVL proteins. (A) FRET between the indicated DsRed-CYB5R proteins and Z-FADS-EGFP or EGFP-Z-FADS. (B) FRET between the indicated DsRed-ELOVL proteins and Z-FADS-EGFP or EGFP-Z-FADS. (C) FRET between the indicated ELOVL-FLAG proteins and Z-FADS-EGFP or EGFP-Z-FADS. Data are the means of five experiments.

Table 1
Distances between fluorophores as determined by fluorescence resonance energy transfer (FRET).

Sample	FRET efficiency (%)	R_0 (Å)	Distance (nm)
Z-FADS-EGFP + DsRed-CYB5R1	N/A	–	–
Z-FADS-EGFP + DsRed-CYB5R2	16 ± 1	63	~8.4
Z-FADS-EGFP + DsRed-CYB5R3	6.0 ± 0.5	63	~9.9
Z-FADS-EGFP + DsRed-ELOVL 2	11 ± 1	63	~8.9
Z-FADS-EGFP + DsRed-ELOVL 4	11 ± 3	63	~9.0
Z-FADS-EGFP + DsRed-ELOVL 5	11 ± 1	63	~9.0
Z-FADS-EGFP + DsRed-ELOVL 7	11 ± 3	63	~8.9
Z-FADS-EGFP + ELOVL 2-FLAG	7.5 ± 1.8	60	~9.1
Z-FADS-EGFP + ELOVL 4-FLAG	13 ± 2	60	~8.3
Z-FADS-EGFP + ELOVL 5-FLAG	32 ± 7	60	~6.9
Z-FADS-EGFP + ELOVL 7-FLAG	N/A	–	–
EGFP-Z-FADS + DsRed-CYB5R1	0.10 ± 0	63	–
EGFP-Z-FADS + DsRed-CYB5R2	8.1 ± 0.5	63	~9.5
EGFP-Z-FADS + DsRed-CYB5R3	9.1 ± 0.5	63	~9.3
EGFP-Z-FADS + DsRed-ELOVL 2	9.7 ± 2.7	63	~9.2
EGFP-Z-FADS + DsRed-ELOVL 4	8.6 ± 0.8	63	~9.4
EGFP-Z-FADS + DsRed-ELOVL 5	2.1 ± 0.8	63	~12
EGFP-Z-FADS + DsRed-ELOVL 7	12 ± 2	63	~8.8
EGFP-Z-FADS + ELOVL 2-FLAG	8.5 ± 2.4	60	~8.9
EGFP-Z-FADS + ELOVL 4-FLAG	3.2 ± 0.4	60	~11
EGFP-Z-FADS + ELOVL 5-FLAG	17 ± 3	60	~7.8
EGFP-Z-FADS + ELOVL 7-FLAG	N/A	–	–
His-ELOVL 2-FLAG	13 ± 1	60	~8.3
His-ELOVL 4-FLAG	11 ± 0	60	~8.5
His-ELOVL 5-FLAG	7.8 ± 0.6	60	~9.1
His-ELOVL 7-FLAG	N/A	–	–

N/A: not available (the distance between the fluorophores may be too great).

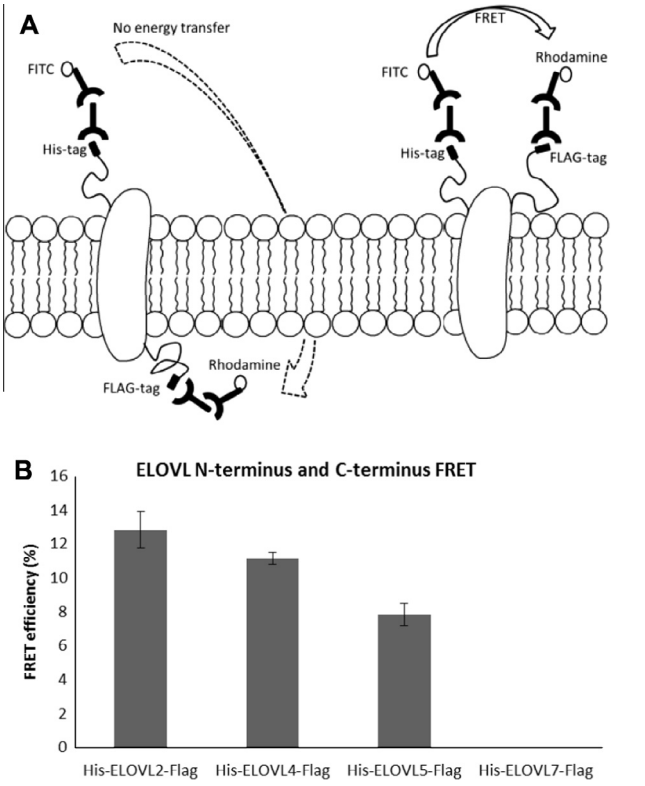

Fig. 3. Orientation of the N- and C-termini of ELOVL transmembrane helices. (A) Diagram depicting the use of ELOVLs tagged at both the N- and C-terminus for determining their relative orientation based on FRET. (B) FRET efficiencies between the N- and C-terminus of the indicated ELOVLs. Data are the means of five experiments.

2.6. Fatty acid analysis

HeLa cells were co-transfected with pcDNA3CF-FADS and pcDNA3CF-ELOVL2, 4, or 5. At 18 h after transfection, HeLa cells were washed with PBS and incubated for 3 h in DMEM containing ALA (5 μg). Cells were subsequently washed and trypsinized. Cellular lipids were extracted with *n*-hexane, as previously described [22]. After treatment of cells with acetyl chloride in methanol, the derived fatty acid methyl esters (FAME) were analyzed by gas chromatography (GC). Fatty acid identity was determined using a Supelco® 37 Component FAME Mix standard (Sigma–Aldrich). The GC system (Agilent HP6890 *plus*) was equipped with a flame ionization detector and a HP-5 capillary column (Agilent). The carrier gas was nitrogen, and the flow rate was 1 mL/min. The initial oven temperature was set at 120 °C and held for 30 min; this was followed by a ramp (3 °C/min) to 250 °C, which was held for a further 20 min; the last step consisted of a final ramp (5 °C/min) to 300 °C, which was maintained for 20 min. The injection port was set at 300 °C in splitless mode.

3. Results

3.1. Z-FADS interacts with CYB5Rs and ELOVLs

HeLa cells were co-transfected with either pEGFP-N1-FADS or pEGFP-C1-FADS, and vectors expressing DsRed-tagged *cyb5r1–3*, *elovl2*, *4*, *5*, or *7*, or FLAG-tagged *elovl2*, *4*, *5*, or *7*, thereby generating

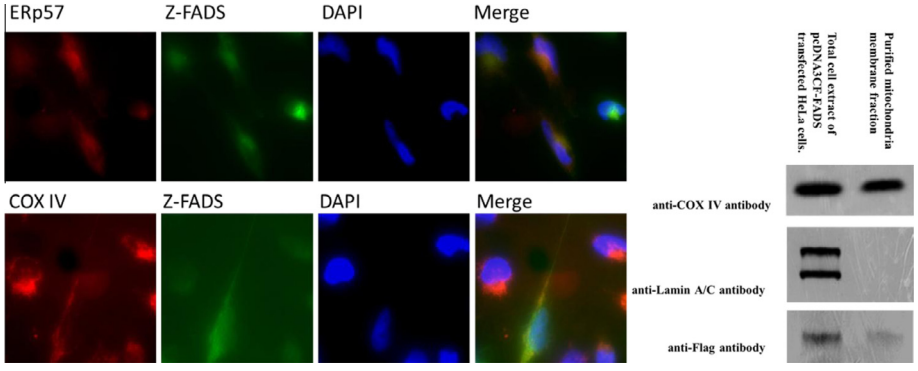

Fig. 2. Sub-cellular localization of Z-FADS. (A) Z-FADS is localized to the endoplasmic reticulum (ER) and mitochondrial membrane, as demonstrated by immunofluorescence cytochemistry. Rabbit anti-ERp57 (marking the ER) and rabbit anti-COX IV (marking the mitochondrial membrane) were recognized by goat anti-rabbit IgG conjugated to Rhodamine (red). Z-FADS was tagged with EGFP (green). Nuclei were stained with DAPI (blue). (B) Western blot analysis. The left lane was loaded with total cellular extract and the right lane was loaded with isolated mitochondrial extract (anti-Lamin A/C was used to confirm the absence of nuclear lamina in the purified fraction). Anti-FLAG M2 was used to probe for Z-FADS-FLAG and anti-COX IV was used to probe for the mitochondrial membrane.

22 combinations. Yellow areas in dual color fluorescence overlay images indicate co-localization of EGFP-Z-FADS (green) and either CYB5R or ELOVL (red) (Fig. S2). Z-FADS does not appear to interact with CYB5R1, but clearly interacts with CYB5R2 and CYB5R3 (Fig. S2A). Z-FADS also interacts with ELOVL2, 4, 5, and 7 (Fig. S2B).

FRET was subsequently used to confirm the observed interactions. The distances between the N-terminus of Z-FADS (the donor) and the N-termini of CYB5R2 and CYB5R3 (the acceptors) were 95 and 93 Å, respectively (Fig. 1A and Table 1). Consistent with the fluorescence microscopy results, FRET was not observed between Z-FADS and CYB5R1. FRET analysis confirmed the interaction between Z-FADS and ELOVLs (2, 4, 5, and 7) (Fig. 1B), with the distance between the Z-FADS C-terminus and the N-termini of ELOVL2, 4, 5, and 7 being 89, 90, 90, and 89 Å, respectively (Table 1). Although FRET was observed between Z-FADS and ELOVL7 tagged with DsRed at the N terminus, it was not observed between Z-FADS and ELOVL7 tagged with FLAG at the C terminus (Fig. 1B and C, Table 1).

3.2. Z-FADS is expressed on the ER and mitochondrial membrane in HeLa cells

To determine the subcellular localization of Z-FADS, we stained HeLa cells expressing Z-FADS with an endoplasmic reticulum (ER) marker, anti-ERp57, and a mitochondrial marker, anti-COX IV. Z-FADS was co-localized with ERp57, suggesting it is present on the ER, as previously speculated [23] (Fig. 2A, upper panel). Z-FADS also co-localized with COX IV, indicating that it resides on the mitochondrial membrane (Fig. 2A, lower panel). This finding was confirmed by subjecting the mitochondrial membrane fraction of HeLa cells to Western blot against Z-FADS (Fig. 2B).

3.3. Modeling of ELOVL transmembrane protein structures

The orientations of the N- and C-termini of ELOVLs were determined by subjecting HeLa cells expressing double-tagged His-ELOVL-FLAG proteins to FRET analysis. A FRET signal is predicted if the N- and C-termini lie on the same side of the ER membrane (either the cytosolic or lumen face) within 1–10 nm of each other (Fig. 3) [24]. The FRET efficiencies for ELOVL2, 4, and 5 were 13 ± 1%, 11 ± 0%, and 7.8 ± 0.6%, respectively. However, FRET was not observed between the N- and C-termini of ELOVL7 (Fig. 3B and Table 1).

3.4. Production of DHA in HeLa cells

To determine whether desaturases other than Z-FADS are required for lipogenesis in zebrafish, HeLa cells were co-transfected with Z-FADS and ELOVL expression vectors, before being incubated with ALA. Fatty acid methyl esters (FAME) were extracted from these HeLa cells and analyzed by GC. The extracted compounds were compared with FAME standards (37 saturated and unsaturated fatty acids of various lengths (C_6–C_{24}); Fig. 4, upper panel). DHA signals were observed in cells co-transfected with the zebrafish *fads* and *elovl* genes (Fig. 4, lower panel), but not untransfected control cells (Fig. 4, middle panel). The incremental production of EPA and DHA are evidenced from the untransfected and transfected HeLa cells. The peak area ratios for (16:1):(18:0):EPA:DHA were changed from 1.0:2.1:0.32:0.18 to 1.0:1.9:0.44:0.27. These results indicate that both EPA and DHA are synthesized in HeLa cells transfected with zebrafish *fads* and *elovl2*, *4*, and *5*.

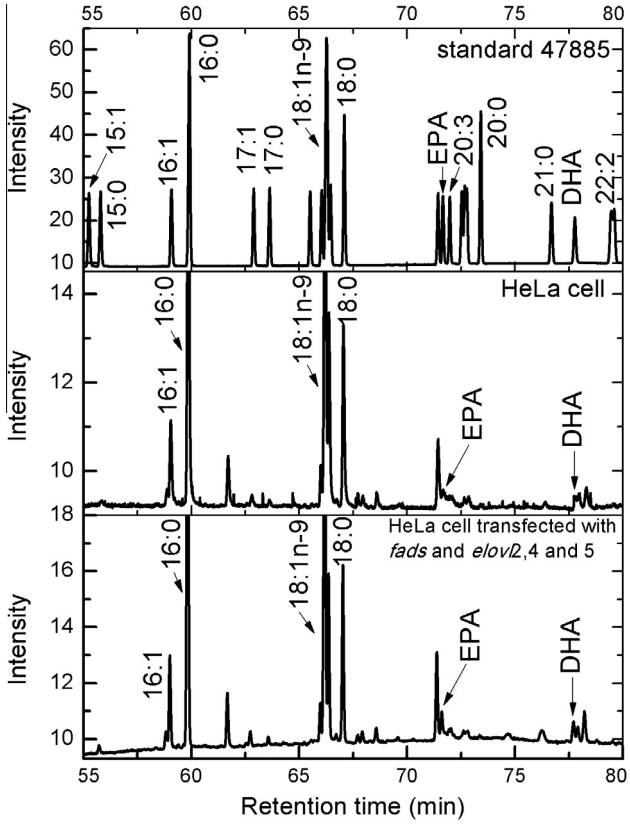

Fig. 4. Gas chromatography analysis of DHA formation. HeLa cells co-transfected with zebrafish *fads* and *elovl2*, *4*, and *5* produced additional EPA (retention time = 71.7 min) and DHA (retention time = 77.8 min). Cells were incubated with ALA. Upper panel: PUFA standard; middle panel: PUFA derived from untransfected HeLa cell extract; lower panel: PUFA derived from transfected HeLa cell extract.

4. Discussion

This study is the first to demonstrate that Z-FADS interacts with CYB5Rs (2 and 3) and ELOVLs (2, 4, 5 and 7), as shown by fluorescence microscopy and FRET. Furthermore, we observed FRET between the respective N- and C-termini of ELOVL2, 4, and 5, indicating that their termini reside on the same side of the lipid bilayer, within 83–91 Å of each other (Fig. 3 and Table 1). FRET was not observed between the N- and C-termini of ELOVL7 (Fig. 3B and Table 1). This suggests that the three-dimensional structure of ELOVL7 in the membrane may be distinct from that of ELOVL2, 4, and 5. The C-terminus of ELOVL7 may be located on the other side of the membrane to the N-terminus, or it may be embedded within the membrane itself. These data will be useful in determining the topology of the ELOVL proteins.

Proteins of the FADS family are known to be distributed on the ER membrane. However, the findings of earlier activity assays suggested that FADS proteins may also be expressed in other organelles [25,26]. Our fluorescence microscopy and Western blot data show that Z-FADS is expressed in the mitochondria (Fig. 2). These results are consistent with an earlier report that FADS1 is expressed in baboon mitochondria [26]. In baboons, alternative splicing generates eleven FADS1 proteins, most of which localize to the mitochondria. On the basis of their common localization, the baboon FADS1 variants and Z-FADS may share similar but yet unidentified roles. This role may be related to beta-oxidation of DHA precursors in mitochondria [19] or peroxisome, which is required for DHA synthesis in most, but not all, biological systems.

Z-FADS has been reported to possess both Δ-5 and Δ-6 activity [15]. Furthermore, ELOVL7 is required for the elongation of C_{18} and

C_{20} PUFAs [27]. Thus, our finding that Z-FADS possibly interacts with the N-terminus of ELOVL7 suggests that these two proteins may be involved in LA and GLA desaturation, and the subsequent elongation required to form C_{20} PUFAs. In rabbits, ELOVL5 is believed to be involved in C_{18}–C_{20} elongation, while ELOVL2 is involved in either C_{18}–C_{20} or C_{20}–C_{22} elongation [28]. Our FRET results indicate that Z-FADS and ELOVL2/5 are in close proximity, further supporting a role for Z-FADS in desaturation during C_{18}–C_{20} elongation [15,25] (Fig. S3). We also demonstrate here that HeLa cells co-transfected with zebrafish *fads* and *elovl2*, *4*, and *5* are able to synthesize DHA (Fig. 4); this finding, combined with the observed interaction between Z-FADS and ELOVL4 (Fig. 1 and S2), and the previous report that zebrafish ELOVL4 elongates LC-PUFAs, including DHA [19], suggests that Z-FADS is involved in DHA biosynthesis through ELOVL4 (Fig. S3). The absence of additional *fads* genes from the zebrafish genome [6,18,29] suggests that Z-FADS may serve as a universal fatty acid desaturase during lipogenesis.

Acknowledgments

This work was supported by the Institute of Cellular and Organismic Biology and the Institute of Chemistry, Academia Sinica, and grants from the National Science Council, R.O.C. (NSC 97-2113-M-001-006-MY3, and 101-2113-M-001-007-MY3 to S.S.-F.Y.). We thank Mr. Bo-Hung Lin of the Taiwan Zebrafish Core Facility at Academia Sinica, Taiwan, for providing the wild type zebrafish AB strain.

Appendix A. Supplementary data

Supplementary data associated with this article can be found, in the online version, at http://dx.doi.org/10.1016/j.bbrc.2013.09.127.

References

[1] J. Tinoco, Dietary requirements and functions of alpha-linolenic acid in animals, Prog. Lipid Res. 21 (1982) 1–45.
[2] R.T. Holman, Control of polyunsaturated acids in tissue lipids, J. Am. Coll. Nutr. 5 (1986) 183–211.
[3] F. Elahian, Z. Sepehrizadeh, B. Moghimi, S.A. Mirzaei, Human cytochrome b5 reductase: structure, function, and potential applications, Crit. Rev. Biotechnol. (2012), http://dx.doi.org/10.3109/07388551.2012.732031.
[4] L.F. Castro, O. Monroig, M.J. Leaver, J. Wilson, I. Cunha, D.R. Tocher, Functional desaturase Fads1 (Delta5) and Fads2 (Delta6) orthologues evolved before the origin of jawed vertebrates, PLoS One 7 (2012) e31950.
[5] A.E. Leonard, S.L. Pereira, H. Sprecher, Y.S. Huang, Elongation of long-chain fatty acids, Prog. Lipid Res. 43 (2004) 36–54.
[6] T. Iyanagi, Redox properties of microsomal reduced nicotinamide adenine dinucleotide-cytochrome b5 reductase and cytochrome b5, Biochemistry 16 (1977) 2725–2730.
[7] L. Spatz, P. Strittmatter, A form of reduced nicotinamide adenine dinucleotide-cytochrome b5 reductase containing both the catalytic site and an additional hydrophobic membrane-binding segment, J. Biol. Chem. 248 (1973) 793–799.
[8] P.G. Passon, D.E. Hultquis, Soluble cytochrome-b5 reductase from human erythrocytes, Biochim. Biophys. Acta 275 (1972) 62–73.
[9] E. Szafer-Glusman, M.G. Giansanti, R. Nishihama, B. Bolival, J. Pringle, M. Gatti, M.T. Fuller, A role for very-long-chain fatty acids in furrow ingression during cytokinesis in *Drosophila* spermatocytes, Curr. Biol. 18 (2008) 1426–1431.
[10] Y. Ohno, S. Suto, M. Yamanaka, Y. Mizutani, S. Mitsutake, Y. Igarashi, T. Sassa, A. Kihara, ELOVL1 production of C24 acyl-CoAs is linked to C24 sphingolipid synthesis, Proc. Natl. Acad. Sci. USA 107 (2010) 18439–18444.
[11] B.G. Fox, K.S. Lyle, C.E. Rogge, Reactions of the diiron enzyme stearoyl-acyl carrier protein desaturase, Acc. Chem. Res. 2004 (2004) 421–429.
[12] J. Shanklin, J.E. Guy, G. Mishra, Y. Lindqvist, Desaturases: emerging models for understanding functional diversification of diiron-containing enzymes, J. Biol. Chem. 284 (2009) 18559–18563.
[13] K. Tamura, D. Peterson, N. Peterson, G. Stecher, M. Nei, S. Kumar, MEGA5: molecular evolutionary genetics analysis using maximum likelihood, evolutionary distance, and maximum parsimony methods, Mol. Biol. Evol. 28 (2011) 2731–2739.
[14] H. Guillou, S. D'Andrea, V. Rioux, R. Barnouin, S. Dalaine, F. Pedrono, S. Jan, P. Legrand, Distinct roles of endoplasmic reticulum cytochrome b5 and fused cytochrome b5-like domain for rat Delta6-desaturase activity, J. Lipid Res. 45 (2004) 32–40.
[15] N. Hastings, M. Agaba, D.R. Tocher, M.J. Leaver, J.R. Dick, J.R. Sargent, A.J. Teale, A vertebrate fatty acid desaturase with Delta 5 and Delta 6 activities, Proc. Natl. Acad. Sci. USA 98 (2001) 14304–14309.
[16] S. Tanomman, M. Ketudat-Cairns, A. Jangprai, S. Boonanuntanasarn, Characterization of fatty acid delta-6 desaturase gene in Nile tilapia and heterogenous expression in *Saccharomyces cerevisiae*, Comp. Biochem. Physiol. B Biochem. Mol. Biol. 166 (2013) 148–156.
[17] S. Ferdinandusse, S. Denis, P.A. Mooijer, Z. Zhang, J.K. Reddy, A.A. Spector, R.J. Wanders, Identification of the peroxisomal beta-oxidation enzymes involved in the biosynthesis of docosahexaenoic acid, J. Lipid Res. 42 (2001) 1987–1995.
[18] Y. Li, O. Monroig, L. Zhang, S. Wang, X. Zheng, J.R. Dick, C. You, D.R. Tocher, Vertebrate fatty acyl desaturase with Delta4 activity, Proc. Natl. Acad. Sci. USA 107 (2010) 16840–16845.
[19] O. Monroig, J. Rotllant, J.M. Cerda-Reverter, J.R. Dick, A. Figueras, D.R. Tocher, Expression and role of Elovl4 elongases in biosynthesis of very long-chain fatty acids during zebrafish *Danio rerio* early embryonic development, Biochim. Biophys. Acta 2010 (1801) 1145–1154.
[20] J.B. Pawley (Ed.), Handbook of Biological Confocal Microscopy, Springer, New York, NY, 2006.
[21] M.R. Wieckowski, C. Giorgi, M. Lebiedzinska, J. Duszynski, P. Pinton, Isolation of mitochondria-associated membranes and mitochondria from animal tissues and cells, Nat. Protoc. 4 (2009) 1582–1590.
[22] A. Masood, K.D. Stark, N. Salem Jr., A simplified and efficient method for the analysis of fatty acid methyl esters suitable for large clinical studies, J. Lipid Res. 46 (2005) 2299–2305.
[23] W.J. Park, H.T. Reardon, C. Tyburczy, K.S. Kothapalli, J.T. Brenna, Alternative splicing generates a novel FADS2 alternative transcript in baboons, Mol. Biol. Rep. 37 (2010) 2403–2406.
[24] D. Maurel, L. Comps-Agrar, C. Brock, M.L. Rives, E. Bourrier, M.A. Ayoub, H. Bazin, N. Tinel, T. Durroux, L. Prezeau, E. Trinquet, J.P. Pin, Cell-surface protein–protein interaction analysis with time-resolved FRET and snap-tag technologies: application to GPCR oligomerization, Nat. Methods 5 (2008) 561–567.
[25] J.P. Infante, V.A. Huszagh, Analysis of the putative role of 24-carbon polyunsaturated fatty acids in the biosynthesis of docosapentaenoic (22:5n-6) and docosahexaenoic (22:6n-3) acids, FEBS Lett. 431 (1998) 1–6.
[26] W.J. Park, K.S. Kothapalli, H.T. Reardon, P. Lawrence, S.B. Qian, J.T. Brenna, A novel FADS1 isoform potentiates FADS2-mediated production of eicosanoid precursor fatty acids, J. Lipid Res. 53 (2012) 1502–1512.
[27] T. Naganuma, Y. Sato, T. Sassa, Y. Ohno, A. Kihara, Biochemical characterization of the very long-chain fatty acid elongase ELOVL7, FEBS Lett. 585 (2011) 3337–3341.
[28] A.E. Leonard, B. Kelder, E.G. Bobik, L.T. Chuang, C.J. Lewis, J.J. Kopchick, P. Mukerji, Y.S. Huang, Identification and expression of mammalian long-chain PUFA elongation enzymes, Lipids 37 (2002) 733–740.
[29] M.K. Gregory, R.A. Gibson, R.J. Cook-Johnson, L.G. Cleland, M.J. James, Elongase reactions as control points in long-chain polyunsaturated fatty acid synthesis, PLoS One 6 (2011) e29662.